

SHARP EDGE EFFECTS ON FRP CONFINEMENT OF RC SQUARE COLUMNS

Raquel Fernandes de Paula, Univ. Nova de Lisboa, PORTUGAL

Manuel Gonçalves da Silva, Univ. Nova de Lisboa, PORTUGAL

Abstract

Shape of cross sections of columns can directly affect the confinement effectiveness of externally bonded FRP jackets. Benefit of strength is higher for circular than for square or rectangular sections. Poor confinement may be due to low FRP jacket stiffness (dependent on type of FRP and number of plies) or to sharp edges in cross-sections. Mitigation of this shape effect is achieved by rounding the corners of rectangular sections with effectiveness increasing with rounding radius, until a certain threshold is reached. A study of the importance of those parameters on the axial compressive behavior of columns was performed by testing a series of RC cylinders and square prisms.

Introduction

Confinement effectiveness of externally bonded FRP jackets depends on different parameters namely type of concrete, steel reinforcement, FRP jacket stiffness (type of FRP, number of plies and design of wrap), shape of cross section, radius of corners, for non-circular sections, and loading conditions. In order to investigate the effect of some of these parameters on the behavior of the columns under axial compression and to quantify the level of confinement exerted on the concrete core, an experimental program has been developed, as described next.

Two types of FRP materials have been utilized in the program: carbon and aramid fibers, both with high tensile characteristics. Carbon fibers have been more commonly applied to reinforce concrete structures, whereas aramid fibers have also proven to be adequate for column confinement, especially to wrap columns with sharp corners. Moreover, the specific properties of aramid fibers (damage tolerance, impact energy absorbance and anti-ballistic properties) make them a more suitable material for certain applications such as to resist vehicle impact on bridge supports or as blast reinforcement of masonry walls (*Pinzelli, 1999*).

The results presented in this paper are for the CFRP wrapped columns, which were tested at the time of submitting the paper. Results obtained showed that stress-strain response of CFRP confined concrete specimens is bilinear, with the second slope being function of the parameter R/D (R – radius of the corners; D - section width). Variation of hoop stresses at mid height of specimens was measured on several gauges bonded to the jacket: in the composite wrap they vary around the perimeter of the section, unlike the case of circular sections. Increase of axial strength and axial and lateral deformation for specimens of circular and square sections are analyzed in the sequel. Published analytical models are also used to generate results compared against experimental data, suggesting modifications on some design procedures.

Experimental Program

Specimens Details

The experimental program consisted of tests performed on 10 series of reinforced concrete cylinders and square prisms of 0.75m height, with an aspect ratio (height/diameter or

width) equal to five. This adopted scaling is explained in [5]. Series definition and details are given in Fig. 1. Each series consisted of 3 identical specimens. The prisms were divided into 3 representative groups: R1 - sharp-edged square section of 0.15m width; R2 - square section with corner radius equal to 20mm; R3 - square section with corner radius equal to 38mm, which corresponds to $\frac{1}{4}$ of the width of the square section. All of the square prisms have the same gross cross sectional area. The radii of the corners were guaranteed by the formwork of the concrete. The longitudinal and transverse reinforcing steel were kept the same for all the column specimens.

Apart from the *reference* specimens, half of the columns were wrapped with 2 plies of carbon unidirectional fibers (CFRP) and the other half with 2 plies of aramid unidirectional fibers (AFRP). The fibers were oriented at 90 degrees to the longitudinal axis of the columns.

Materials

High strength carbon fibers used in this study, namely *Mbrace FRP CI-30*, had mechanical properties of the CFRP determined by tensile tests on flat coupons as per ASTM D3039. CFRP materials exhibited linear – elastic behavior up to failure. The tensile strength (f_{uj}) and modulus (E_j) were equal to 4198MPa and 228.8GPa, respectively. Ultimate strain was determined to be 1.76% (ϵ_{uj}). The manufacturer’s data are also presented for comparison: $f_{uj} > 3400$ MPa; $E_j = 240$ GPa; $\epsilon_{uj} = 1.55\%$. The compressive strength of concrete after 28 days was $f_c = 27.5$ MPa.

Instrumentation and Testing

To measure axial strain (by measuring displacement), 2 or 3 LVDTs were used. Lateral strains (CFRP strains) were tracked on several gauges that were bonded horizontally at the mid-height of each specimen. The tests were conducted with an electro-hydraulic universal testing machine, which has a vertical load capacity of up to 3000kN, at a controlled rate of axial displacement of 0.01mm/sec.

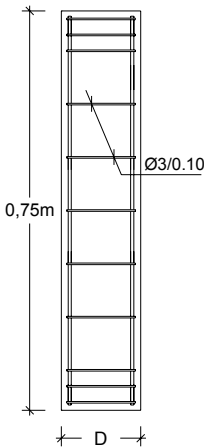

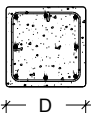
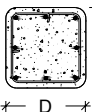

Elevation	Cross section	Diameter/ Width D(m)	Corner radius R(mm)	Series		
				Unconfined	Confined with CFRP	Confined with AFRP
 <p>0.75m</p> <p>Ø3/0.10</p> <p>Long. reinf.: 8Ø6 Stirrups: Ø3/0.10</p>	 <p>← D →</p>	0.15	-	CNR	CC	CA
	 <p>← D →</p> <p>↑ D ↓</p>	0.15	-	QR1NR	QR1C	QR1A
	 <p>← D →</p> <p>↑ D ↓</p> <p>R2</p>	0.151	20	-	QR2C	QR2A
	 <p>← D →</p> <p>↑ D ↓</p> <p>R3</p>	0.154	38	-	QR3C	QR3A

Figure 1. Series details: geometry, reinforcement and type of confinement

Experimental Results and Analysis

Compression behavior of the CFRP wrapped specimens was very similar in each series in terms of stress-strain curves and failure modes of the specimens. Failure of all of the CFRP confined specimens occurred in a sudden and explosive way and was only preceded by the discoloration of the resin and some creeping sounds. In some cases it was also possible to observe the *debonding* of small widths of the end zone of the overlapping fibers. Two specimens after failure are presented in Fig. 3.

A selection of typical stress – strain curves for each series of experiments is shown in Fig. 2. The curves of the CFRP confined concrete are bilinear with a transition zone, except in the case of the sharp edge columns. In this text the first slope of the curve will be referred to as the initial elastic zone with initial rigidity equal to E_1 and the second slope as the final plastic zone with rigidity E_2 . The elastic slope is not substantially altered with confinement, as it is identical to that of the unconfined concrete. The transition zone occurs shortly after the peak strength of the unconfined concrete (*reference* specimens) has been reached. The plastic rigidity (E_2) is function of the geometry of cross section. As expected, the strength of confined columns is higher for circular sections than for square ones. Also, efficiency of CFRP confinement of square columns increases with decreasing corner sharpness.

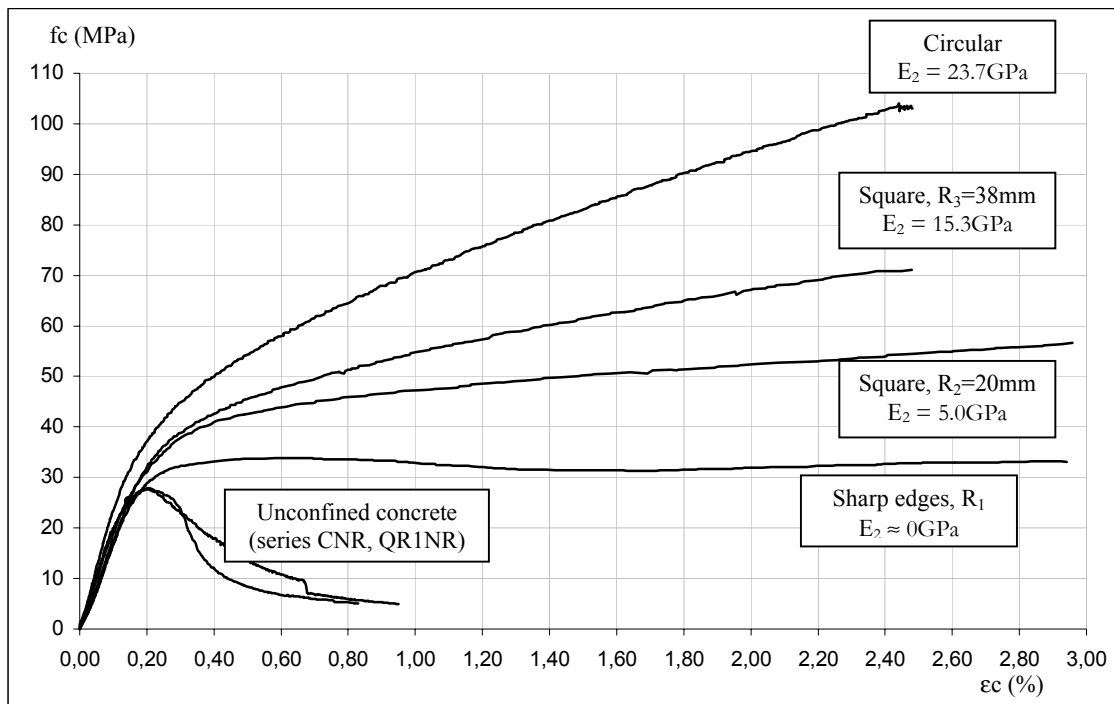


Figure 2. Stress - strain curves of CFRP confined square and circular RC columns

Axial Compressive Strength and Axial Strain at Failure

Table 1 summarizes the results in terms of increase of ultimate axial compressive strength and strain, with relation to *reference* specimens. Compression stresses and strains are mean values for each series. The following conclusions may be drawn:

- The efficiency of the CFRP confinement is higher for circular than for square sections, as expected.

- The radius of the corners of square sections is of great importance in relation to the level of confinement:
 - The increase of ultimate strength of sharp edged sections is low, although there is a certain gain of load capacity and of ductility;
 - Corner radii of 20mm and 38mm determine a much higher gain of load capacity, with effectiveness increasing with rounding radius.
- The increase of axial deformation is very high for all the considered geometries.

Table 1. Increase of ultimate axial compressive strength and strain of confined CFRP specimens

Series	f_{cu}	ϵ_{cu}	f_{cu}/f_{cu}^1	$\epsilon_{cu}/\epsilon_{cu}^1$
	(MPa)	(%)		
CNR	27.8	0.209	1.00	1.00
CC	103.4	2.551	3.72	12.2
QR1NR	27.1	0.225	1.00	1.00
QR1C	32.6	2.439	1.20	10.8
QR2C	53.0	2.751	1.96	12.2
QR3C	68.6	1.982	2.53	8.8

Note:
 1 – mean values of the *reference* specimens: series CNR and QR1NR (circular and square sections, respectively)

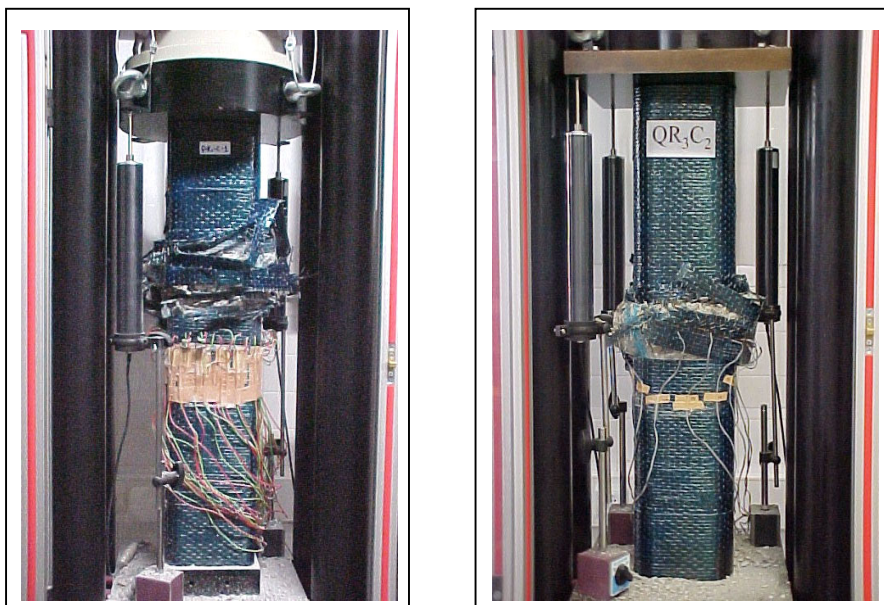


Figure 3. Specimens QR2C1 and QR3C2 after failure

Lateral Strain / CFRP Strain at Failure

The ultimate strength of the confined concrete is closely related to the failure strength of the FRP wraps. CFRP strain at rupture of the confined columns is usually lower than the ultimate strain obtained by tensile testing of the CFRP coupons. This reduction is due to several reasons, including the curved shape of the CFRP wrap, especially at corners with low radius (Davol, 1998).

For the CFRP wrapped cylinders, the maximum lateral strain obtained was equal to 1.45%, which is lower than the CFRP tensile strength. Unlike those in the circular sections, the lateral stresses in the square specimens vary around the section. Figure 5 shows the variation of the CFRP strain (lateral strain) along the perimeter of the section of specimen QR2C1. The evolution of the CFRP strain is plotted against the values $f_c - \epsilon_c$, at selected points of the perimeter of the section where the gauges were glued to the CFRP. For each side of the square specimen, maximum values of CFRP extension occurred at the start of the curved segment (these values are presented in Fig. 5). The rupture of the specimen corresponded to a maximum extension of the CFRP of 1.63% (gauge 5), which corresponds to a tensile stress of 3729.4MPa, i. e., about 88.8% of its tensile strength.

After the initial elastic phase, the outer ply of the fibers started to *debond* at the end zone of overlapping. The gauges bonded in that zone denoted this phenomenon, as the CFRP extension decreased and reached negative values (compression). The first gauge to register the decrease of the extension was the 21st, followed consecutively by the 20, 19 and 18. At one of the corners of this specimen (gauge 22) negative values of the CFRP strain were also registered.

The sequence of the principal characteristics of the failure mode of this series (QR2C) is illustrated in Fig. 4: first, the *debonding* of the end zone of overlapping and then, immediately after maximum force was achieved, the rupture of the fibers at one of the corners of the specimen. Observation of the specimens after the tests permitted to verify that the rupture of the fibers occurred at the start of the curved segment and to observe the curvature of the longitudinal bars between stirrups.

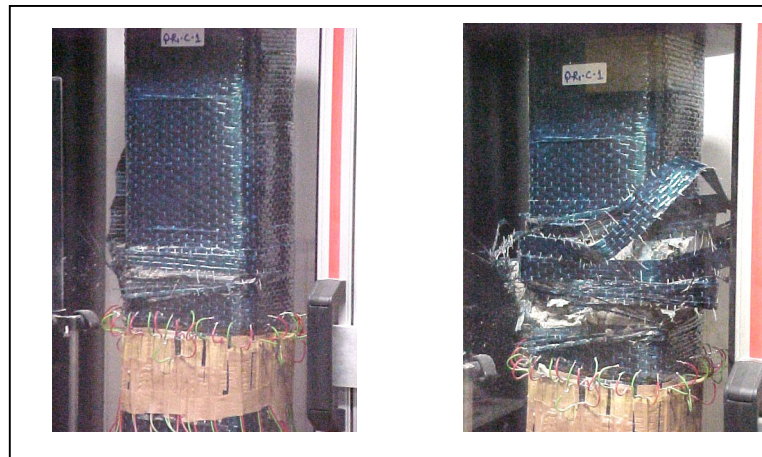


Figure 4. Illustration of failure mode of specimen QR2C (corner radii equal to 20mm)

Similar plots to that in Fig. 5 have been obtained for each square CFRP confined specimen but they are not presented here for brevity. However, maximum CFRP strains at different locations along the perimeter of the square sections are shown in Table 2. From this table, it can be seen that the maximum tensile strain occurred at the center of the flat or near the

start of the radius for the specimens with rounded corners, except for the specimen QR3C3. It has been referred that as the concrete expands the flat sides bulge out and the final section resembles a circular section as the loading progresses. This deformed section is better able to resist further expansion than the original geometry (*Davol, 1998*).

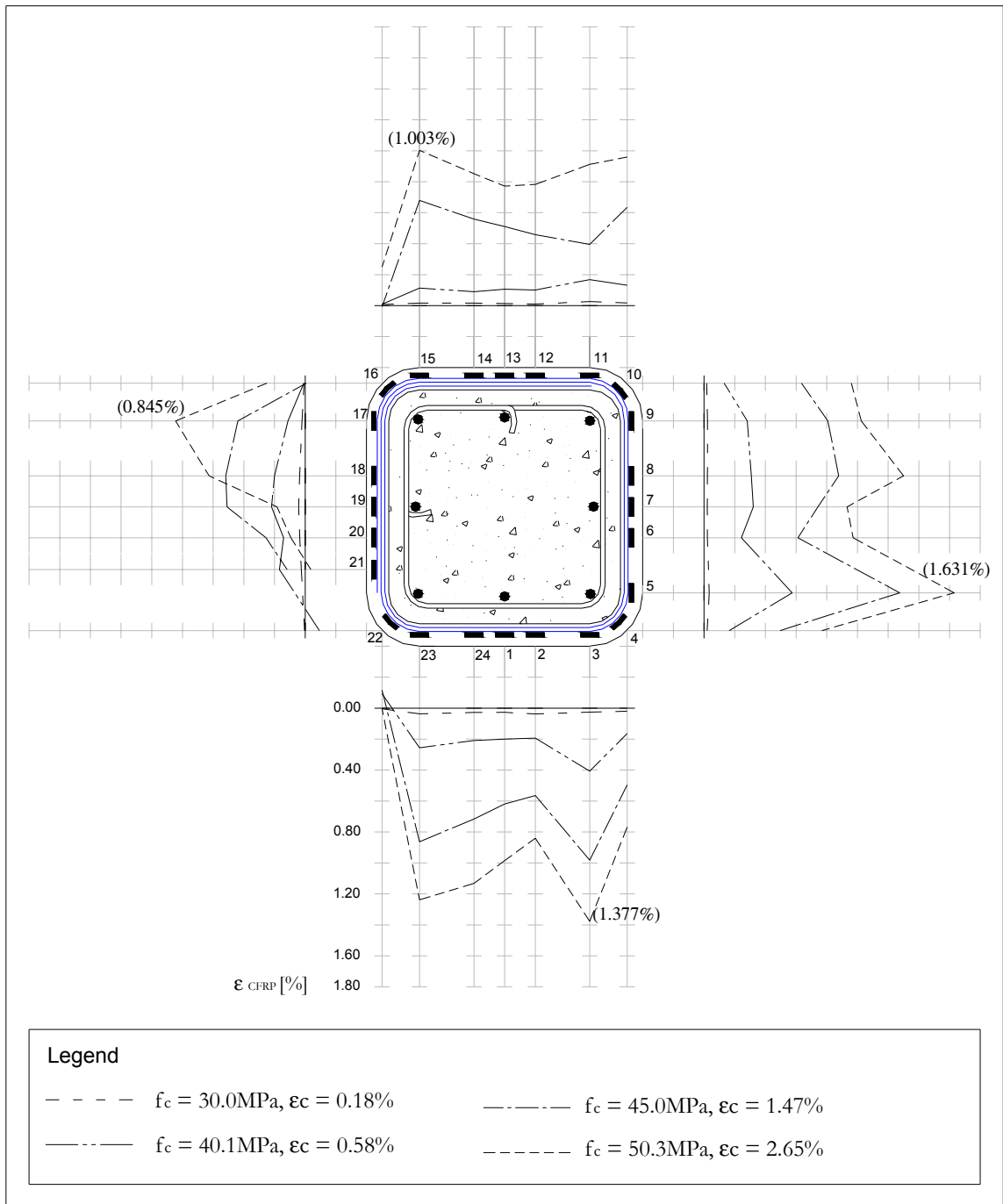


Figure 5. CFRP strain along the perimeter of specimen QR2C1 (function of $f_c - \epsilon_c$)

For the sharp edged sections, the maximum CFRP strains occurred near the corners and did not engage CFRP tensile tested capacity. CFRP strain values of the sharp-edged CFRP confined columns indicate that the confining mechanism has not been fully activated. Typical shape of the stress-strain curves of sharp-edged CFRP confined columns indicates that the geometry of cross section does not allow the CFRP wrap to develop sufficient confining pressure to overcome the effect of the degradation of the concrete under the large strains it experiences after the initial elastic zone.

Table 2. Variation of CFRP strain around the perimeter of square sections

Series	Specimens	Maximum CFRP strain (%)		
		Center of flat side	~1.5cm away from the corner	
QR1C	QR1C1	0.851	1.151	
	QR1C2	0.249	0.389	
	QR1C3	0.107	0.155	
		Center of flat	Start of curve	Corner
QR2C	QR2C1	0.960	1.631	0.960
	QR2C2	1.250	1.113	1.110
	QR2C3	1.581	1.017	0.914
QR3C	QR3C1	0.870	0.718	0.833
	QR3C2	1.608	1.683	1.008
	QR3C3	1.101	0.779	1.140

Note: CFRP strains correspond to failure of the specimens.

Numerical Study

Several models that evaluate the FRP confined concrete properties have been assessed against the experimental database presented in this paper. A review of predictive equations to calculate the ultimate compressive strength and strain is presented in *Lam and Teng (2001)*. The entire stress-strain diagrams can be obtained from different proposed models as summarized in *Manfredi and Realfonzo (2001)*.

Most of the existing models have been applied to cylindrical sections. To predict the FRP confined properties of concrete square sections, an effective lateral confining pressure was determined by introducing a confinement effectiveness coefficient (k_e), which is obtained by considering the ratio Ae/Ac , where Ae is the area of effectively confined concrete core and Ac is the area of concrete (gross cross-sectional area minus area of longitudinal steel reinforcement). For a square section, k_e takes into account the radius of the corners and is given by equation: $k_e = 1 - 2(b - 2R)^2 / 3A_g$, where b is the width of the square section and R is the radius of corners.

Some of the existing models have been found to match experimental results more closely than others. In Figs. 6 to 8, the theoretical stress – strain diagrams of the CFRP confined concrete columns, calculated using an incremental - iterative model proposed by *Spoelstra and Monti (1999)* and a modified version of such model proposed by *Manfredi and Realfonzo (2001)*, are

plotted against the experimental data. The ultimate strain of the CFRP jacket was equal to that determined by tensile test of flat coupons.

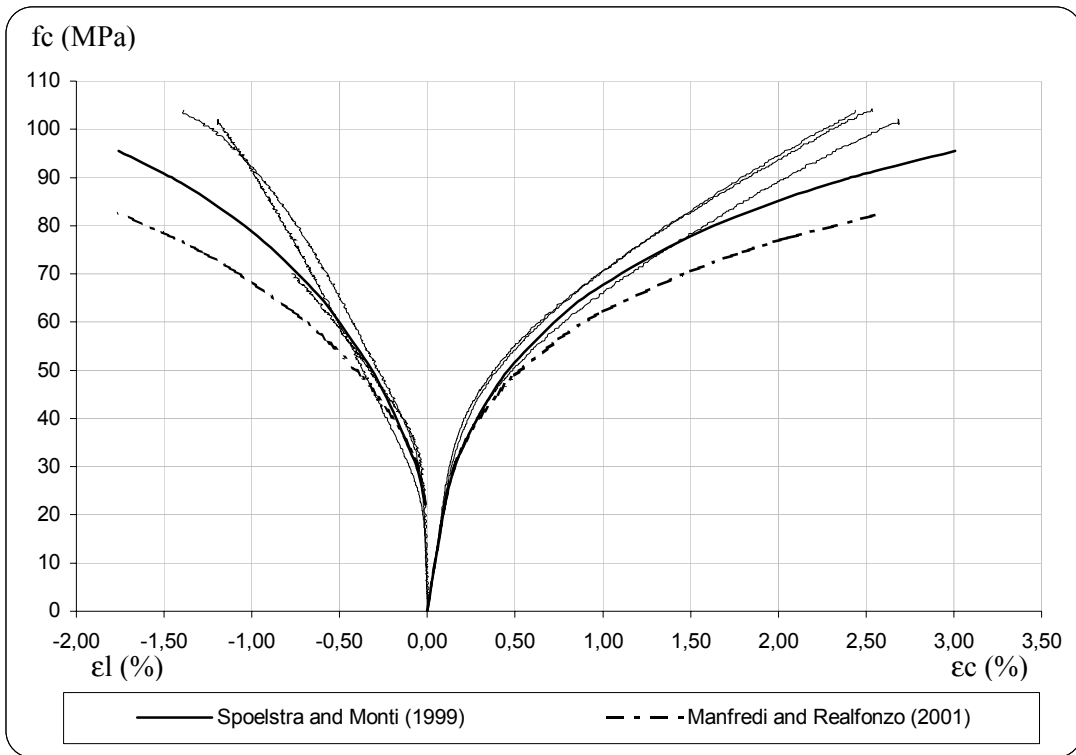


Figure 6. Series CC – circular section: experimental versus *SM* and *MR* curves

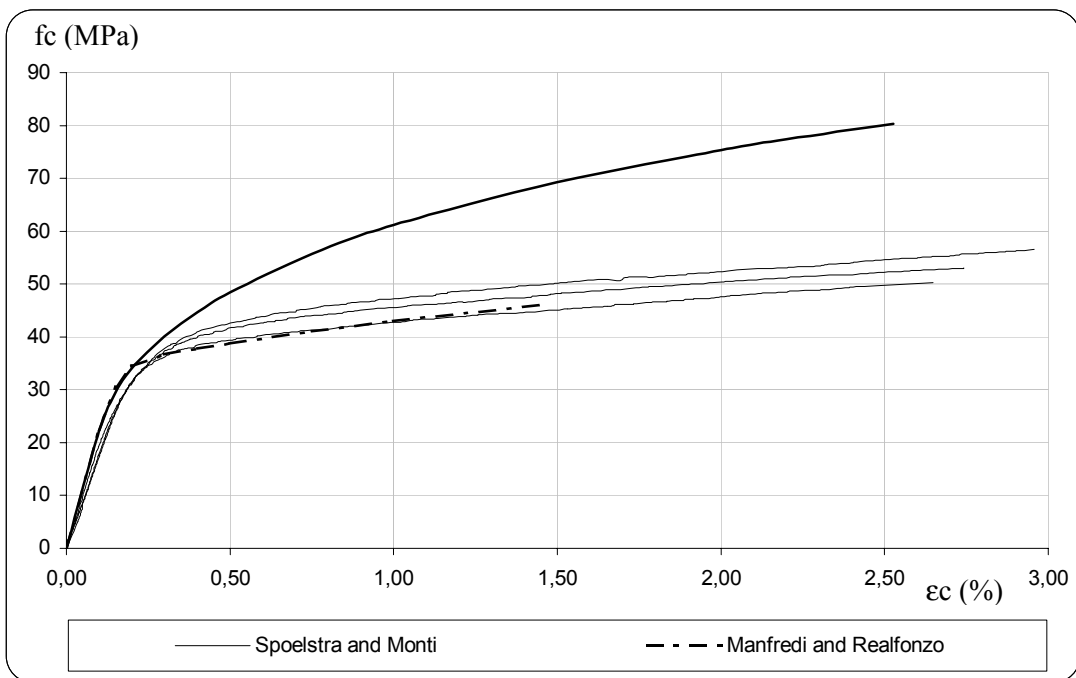


Figure 7. Series QR2C – Square, $R_2 = 20\text{mm}$: experimental versus *SM* and *MR* curves

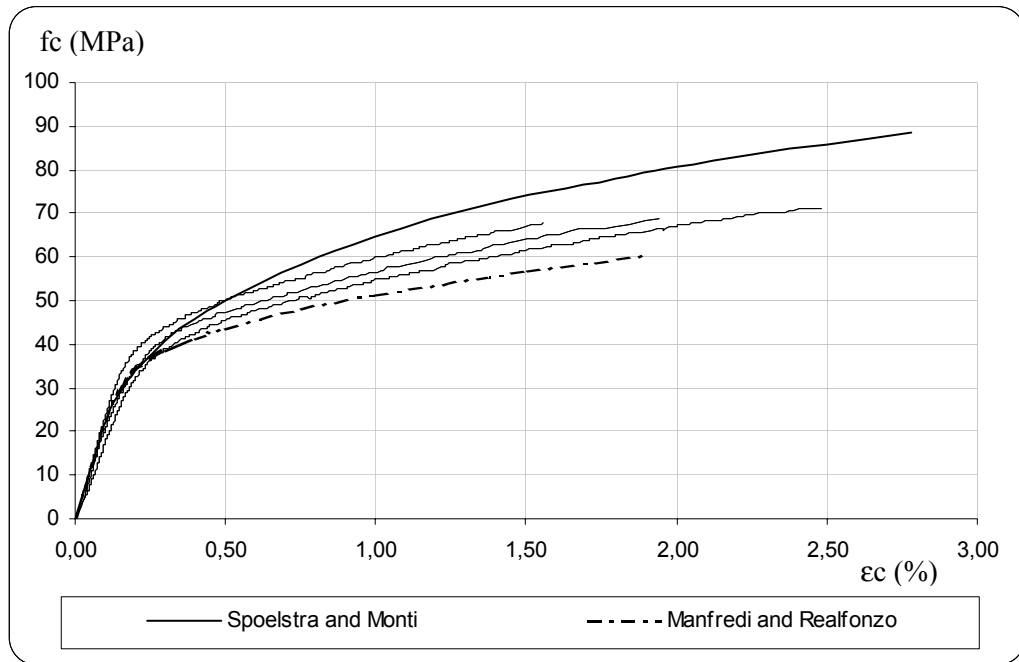


Figure 8. Series QR3C – Square, $R_3 = 38\text{mm}$: experimental versus *SM* and *MR* curves

A satisfactory agreement between experimental and predicted *SM* curves can be observed for the circular (series CC) specimens. On the other hand, the estimated values of E_2 and of ultimate strength by *MR* model are lower than the experimental ones. For the square specimens there is a significant discrepancy between proposed and experimental data. Only for QR2C series ($R_2=20\text{mm}$) the estimated value of E_2 by *MR* model is close to the experimental mean one. However, ultimate strain is much lower than the experimental values. For the maximum radius series (QR3C), both models set bounds for the experimental results.

Table 3 – Comparison between experimental results and theoretical models

Series	<i>Spolstra and Monti (1999)</i>				<i>Manfredi and Realfonzo (2001)</i>			
	f_{cc}^{teo} (MPa)	$f_{cc}^{exp}/f_{cc}^{teo}$	ϵ_{cc}^{teo} (%)	$\epsilon_{cc}^{exp}/\epsilon_{cc}^{teo}$	f_{cc}^{teo} (MPa)	$f_{cc}^{exp}/f_{cc}^{teo}$	ϵ_{cc}^{teo} (%)	$\epsilon_{cc}^{exp}/\epsilon_{cc}^{teo}$
CC	95.6	1.08	3.006	0.85	82.6	1.25	2.599	0.98
QR2C	79.7	0.66	2.507	1.11	46.1	1.15	1.450	1.92
QR3C	88.6	0.77	2.788	0.71	60.5	1.13	1.904	1.04

Conclusions

Uniaxial compression tests on RC columns confined with CFRP jackets have shown that the increase of ultimate strength is highly influenced and increases with the radius of the corners of square sections. On the other hand, the increase of axial deformation capacity is up to 8 times that of unconfined concrete, even for the sharp edged sections.

Further investigation is required in order to calibrate models capable of predicting actual behavior of FRP confined concrete including geometric parameters need to be included in equations.

Experimental work on jackets made with aramid fibers are expected to shed further light on alternatives that mitigate problems caused by sharp edges of columns

Acknowledgments

The authors are grateful to Mr. José Gaspar and Alexandre Paulo for their precious help with the lab experiments. Special thanks are due to Mr. Carlos Rodrigues for his contribution to the execution of the experimental testing setup.

The Portuguese Foundation for Science and Technology provided support for this study under PRAXIS XXI Project CEG 3/3.1/2572-95.

References

1. ASTM D3039, "Standard test method for tensile properties of polymer matrix composite materials", Vol. 14.02, 1995.
2. Davol, A., "Structural Characterization of Concrete Filled Fiber Reinforced Shells", University of California, San Diego, 1998.
3. Lam, L. and Teng, J. G., (2001), "Strength models for circular concrete columns confined by FRP composites", *FRPRCS-5*, Thomas Telford, London
4. Manfredi, G. and Realfonzo, R., "Models of concrete confined by fiber composites", *FRPRCS-5*, Thomas Telford, London, 2001
5. Pinzelli R., "The contribution and role of aramid fibre for external strengthening and repairs of concrete structures", *Structural Faults & Repair 99 Conference*
6. Rodrigues, C. C., Silva, M. G., "Experimental Investigation of CFRP Reinforced Concrete Columns under Uniaxial Cyclic Compression", *FRPRCS-5*, Thomas Telford, London, 2001
7. Spoelstra, M. R. and Monti, G., (1999), "FRP – Confined concrete model", *Journal of Composites for Construction*, ASCE, 3, 143-150